Inorganica Chimica Acta xxx (2016) xxx–xxx

Contents lists available at ScienceDirect

Inorganica Chimica Acta

journal homepage: www.elsevier.com/locate/ica

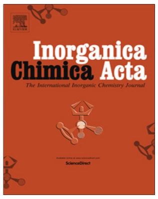

Research paper

# Synthesis and characterization of iron and cobalt complexes with an asymmetric *N*-alkyl,*N*′-aryl-β-diketiminate ligand

Erwin A. Weerawardhana [a], Andres Pena [a], Matthias Zeller [b], Wei-Tsung Lee [a,*]

[a] *Department of Chemistry and Biochemistry, Loyola University Chicago, Chicago, IL 60660, United States*
[b] *Department of Chemistry, Purdue University, West Lafayette, IN 47907, United States*

ARTICLE INFO

*Article history:*
Received 10 June 2016
Accepted 28 June 2016
Available online xxxx

*Keywords:*
Iron complex
Cobalt complex
Low-valent
Asymmetric beta-diketiminate

ABSTRACT

An asymmetric *N*-alkyl,*N*′-aryl-β-diketiminate ligand L (L = 2-((S)-(-)-1-phenylethylimino)-4-(2,6-diisopropylphenylimido)pentane) was prepared. Synthesis of solvent-free chloro-bridged dimers, $[LFe(\mu\text{-}Cl)]_2$ and $[LCo(\mu\text{-}Cl)]_2$ are presented. Upon reduction in the presence of *cis*-cyclooctadiene, rare examples of low-valent complexes LFe(cod) and LCo(cod) were obtained. All metal complexes were fully characterized by $^1$H NMR spectroscopy, elemental analysis, and X-ray crystallography. Crystallographic and spectroscopic results indicate that the *N*-alkyl,*N*′-aryl-β-diketiminate ligand L is sterically smaller but a better electron donor than the *N*,*N*′-diaryl-substituted β-diketiminate ligand $L^{Me,Dipp}$ ($L^{Me,Dipp}$ = 2,4-bis(2,6-diisopropylphenylimido)pentane).

## 1. Introduction

Since discovery in 1968 [1], β-diketiminates have been widely used as supporting ligands in organometallics and coordination chemistry, which, in part, is due to their facile steric and electronic tunability [2–4]. Most metal complexes with coordinating β-diketiminates (derived from acetylacetonate) were based on symmetrical substituents, e.g. *N*,*N*′-diaryl- and *N*,*N*′-dialkyl-β-diketiminates (Fig. 1) [2]. One of the reasons is synthetic simplicity – one condensation reaction is needed for ligand preparation. Metal complexes with smaller *N*,*N*′-dialkyl substituents are often used in chemical vapor deposition and atomic layer deposition [5,6], while studies have revealed that metal complexes with bulkier *N*-substituted dialkyl ligands are capable of catalyzing ring-opening polymerizations [7,8] and olefin polymerizations [9,10]. In addition, complexes of *N*,*N*′-diaryl-β-diketiminates have shown versatile reactivity, such as small molecule activation [11,12], cross-coupling reactions [13], and polymerization reactions [14,15].

In light of these findings, a new class of metal complexes supported by asymmetric β-diketiminates with *N*-alkyl,*N*′-aryl substitution could open a new avenue for chemistry of metal complexes with β-diketiminates. Asymmetric ligands should allow for fine tuning the steric hindrance around the metal center, since two independently modifiable substituents are accessible. Chiral information can also be easily installed on the ligands, as many chiral aliphatic primary amines are commercially available. However, reports using such bidentate asymmetric β-diketiminates in the synthesis of metal complexes are scarce [16–20].

In the present work, we report the synthesis and characterization of well-defined M(II) and M(I) (M = Fe and Co) complexes with an asymmetric *N*-alkyl,*N*′-aryl β-diketiminate. The steric and electronic effects are compared with those of symmetrical *N*,*N*′-diaryl β-diketiminates supporting metal complexes.

## 2. Experimental

### 2.1. Material and methods

All manipulations were performed under a nitrogen atmosphere using standard Schlenk techniques or in an M. Braun Labmaster glovebox. Glassware was dried at 150 °C overnight. Diethyl ether, *n*-pentane, tetrahydrofuran, and toluene, were purified by the Glass Contour solvent purification system. Deuterated benzene was first dried with $CaH_2$, then over Na/benzophenone, and then vacuum transferred into a storage container. Before use, an aliquot of each solvent was tested with a drop of sodium benzophenone ketyl in THF solution. All reagents were purchased from commercial vendors and used as received. 2-(2,6-Diisopropylphenylimido)-2-pentene-4-one was prepared according to a literature procedure [21]. $^1$H NMR data were recorded on Varian Inova 300 or 500 MHz spectrometer at 22 °C. Resonances in the $^1$H NMR spectra are referenced either to residual $CHCl_3$ at $\delta = 7.26$ ppm or

---

* Corresponding author.
*E-mail address:* wlee5@luc.edu (W.-T. Lee).

http://dx.doi.org/10.1016/j.ica.2016.06.039

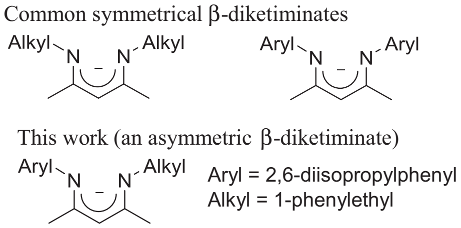

**Fig. 1.** β-Diketiminates derived from acetylacetonate.

$C_6D_5H$ at $\delta = 7.16$ ppm. Solution magnetic susceptibilities were determined by the Evans method [22]. UV–visible spectra were recorded on an Agilent Cary 8454 UV–vis spectrophotometer. Fourier transform-infrared (FTIR) spectroscopy was performed using a Shimadzu IRAffinity-1S, FTIR spectrometer. Elemental analysis was conducted by Midwest Microlab, LLC (Indianapolis, IN).

### 2.2. Synthesis of 2-((S)-(-)-1-Phenylethylimino)-4-(2,6-diisopropyl phenylamido)pent-2-ene (HL)

4.7 g (38.6 mmol) of (S)-(-)-1-phenylethylamine, 10 g (38.6 mmol) of 2-(2,6-diisopropylphenylimido)-2-pentene-4-one, catalytic amounts of *p*-toluenesulfonic acid monohydrate, and 200 mL of toluene were combined in a round bottomed flask. A Dean–Stark apparatus was attached and the solution brought to reflux for 4 d. Volatiles were removed under reduced pressure and the residue was extracted with 100 mL of dichloromethane. After removing of solvent, the resulting dark oil was redissolved in 50 mL of ethanol and 20 mL of 6 M hydrochloric acid. The off-white precipitate was collected by filtration and then treated with 150 mL of diethyl ether and 150 mL of saturated $Na_2CO_3$ solution. The mixture was stirred until all solids had redissolved. The water layer was removed and extracted with 3 × 50 mL of ether. The combined organic layers were dried over anhydrous $MgSO_4$, filtered, and evaporated under reduced pressure to give a yellow oil, which was crystallized from a concentrated *n*-hexane solution (7.3 g, 52%). $^1H$ NMR (300 MHz, $CDCl_3$, $\delta$): $\delta$ 11.40 (br, 1H, N*H*), 7.41–7.09 (m, 8H, Ar*H*), 4.78–4.72 (m, 1H, NC*H*(Me)Ph, 4.75 (s, 1H, *H*C{C(Me)NR}$_2$), 3.15–2.99 (m, 2H, C*H*Me$_2$), 1.92 (s, 3H, HC{C(C*H*$_3$)NR}$_2$), 1.73 (s, 3H, HC{C(C*H*$_3$)NR}$_2$), 1.49 (d, 3H, *J* = 6.6 Hz, NCH(C*H*$_3$)Ph), 1.32–1.23 (m, 12H, ArCH(C*H*$_3$)$_2$). Anal. Calcd for $C_{25}H_{34}N_2$: C 82.82, H 9.45, N 7.73. Found: C 82.88, H 9.58, N 7.88.

### 2.3. Synthesis of [LFe(μ-Cl)]$_2$ (**1**)

To a stirred solution of HL (500 mg, 1.38 mmol) in diethyl ether (3 mL) at ambient temperature under $N_2$ atmosphere was added a solution of LDA (155 mg, 1.45 mmol) in diethyl ether (2 mL) for 2 h. Solid $FeCl_2(THF)_{1.5}$ (340 mg, 1.45 mmol) was added, and the resulting slurry was stirred for 18 h at ambient temperature. Volatiles were removed under reduced pressure, and the residue was extracted with toluene and filtered through Celite. The filtrate was dried in *vacuo* to yield an orange solid (570 mg, 91%). Crystals suitable for X-ray diffraction were grown from a concentrated solution in n-pentane at −35 °C. $^1H$ NMR (300 MHz, $C_6D_6$, $\delta$): 11, 10, 4.8, 4.6, 0.8, −1.1, −8.5 (br), −14 (br), −26, −29, −34 (br), −40, −45. $\mu_{eff}$ ($C_6D_6$): 6.2 ± 0.4 $\mu_B$. Anal. Calcd for $C_{50}H_{66}N_4Cl_2Fe_2$: C, 66.31; H, 7.35; N, 6.19. Found: C, 66.53; H, 7.21; N, 6.04.

### 2.4. Synthesis of LFe(cod) (**2**)

To 100 mg (0.11 mmol) of [LFe(μ-Cl)]$_2$ and 120 mg (01.10 mmol) of *cis*-cyclooctadiene suspended in *n*-pentane (15 mL) at ambient temperature under $N_2$ atmosphere was added 59 mg (0.44 mmol) of $KC_8$. The resulting slurry was stirred for 3 d at ambient temperature. The reaction mixture was filtered through Celite. The filtrate was dried in *vacuo*, and the residue was extracted with *n*-pentane (20 mL) to obtain an olive green solution. Volatiles were removed under reduced pressure to afford a yellow-green solid (62 mg, 29%). Crystals suitable for X-ray diffraction were grown from a concentrated *n*-pentane solution of the complex at −35 °C. $^1H$ NMR (300 MHz, $C_6D_6$, $\delta$): 10, 9.4, 6.8, 6.6, 5.2, 2.6, 2.2, 1.2, −0.7, −1.3, −8.0 (br), −43. $\mu_{eff}$ ($C_6D_6$): 3.7 ± 0.3 $\mu_B$. UV–vis (THF): 600 ($\varepsilon = 110\ mM^{-1}\ cm^{-1}$), 930 ($\varepsilon = 85\ mM^{-1}\ cm^{-1}$). Anal. Calcd for $C_{33}H_{45}N_2Fe$: C, 75.41; H, 8.63; N, 5.33. Found: C, 75.49; H, 8.69; N, 5.27.

### 2.5. Synthesis of [LCo(μ-Cl)]$_2$ (**3**)

To a stirred solution of HL (500 mg, 1.38 mmol) in diethyl ether (3 mL) at ambient temperature under $N_2$ atmosphere was added a solution of LDA (155 mg, 1.45 mmol) in diethyl ether (2 mL) for 2 h. Solid $CoCl_2$ (188 mg, 1.45 mmol) was added, and the resulting slurry was stirred for 18 h at ambient temperature. Volatiles were removed under reduced pressure, and the residue was extracted with toluene and filtered through Celite. The filtrate was dried in *vacuo* to yield a dark brown solid (595 mg, 87%). Crystals suitable for X-ray diffraction were grown from a concentrated solution in *n*-pentane at −35 °C. $^1H$ NMR (300 MHz, $C_6D_6$, $\delta$): 18, 17, 4.2, 3.8, 2.7, 1.9, −4.6 (br), −20, −23, −32 (br), −33, −36, −42. $\mu_{eff}$ ($C_6D_6$): 5.8 ± 0.3 $\mu_B$. Anal. Calcd for $C_{50}H_{66}N_4Cl_2Co_2$: C, 65.86; H, 7.30; N, 6.14. Found: C, 65.88; H, 7.35; N, 6.26.

### 2.6. Synthesis of LCo(cod) (**4**)

To 100 mg (0.11 mmol) of [LCo(μ-Cl)]$_2$ and 120 mg (01.10 mmol) of *cis*-cyclooctadiene suspended in *n*-pentane (15 mL) at ambient temperature under $N_2$ atmosphere was added 59 mg (0.44 mmol) of $KC_8$. The resulting slurry was stirred for 3 d at ambient temperature. The reaction mixture was filtered through Celite. The filtrate was dried in *vacuo*, and the residue was extracted with *n*-pentane (20 mL) to obtain an olive green solution. Volatiles were removed under reduced pressure to afford a red orange solid (66 mg, 25%). Crystals suitable for X-ray diffraction were grown from a concentrated *n*-pentane solution of the complex at −35 °C. $^1H$ NMR (300 MHz, $C_6D_6$, $\delta$): 33 (br), 18, 10.4, 10.3, 6.4, 6.3, 2.7, 2.2, 1.8, 0.5 (br), −1.8, −3.2, −16 (br), −22, −24, −25, −67 (br). $\mu_{eff}$ ($C_6D_6$): 3.2 ± 0.4 $\mu_B$. UV–vis (THF): ~480 (sh) ($\varepsilon = 590\ mM^{-1}\ cm^{-1}$). Anal. Calcd for $C_{33}H_{45}N_2Co{\cdot}THF$: C, 73.97; H, 8.89; N, 4.66. Found: C, 73.73; H, 8.12; N, 4.59.

### 2.7. Solid angle calculations

Solid angle calculations were performed using the program Solid-G [23]. The ligand coordinates used in the calculations were taken from X-ray crystal structure data. The metal ligand bond lengths were set at a distance of 2.28 Å. In cases where there was more than one molecule in the asymmetric unit, solid angles were calculated for each molecule, and the average value is reported.

### 2.8. Crystallography

Data were collected using either a Bruker-Nonius KappaCCD (**1**, **3**–**5**) or a Quest CMOS diffractometer (**2**) with Mo-K$_\alpha$ radiation ($\lambda = 0.71073$ Å). The KappaCCD instrument features a fine focus sealed tube X-ray source with graphite monochromator. The Quest CMOS instrument is equipped with IμS microsource with a laterally graded multilayer (Goebel) mirror for monochromatization. Single crystals were mounted on Mitegen loop or micromesh mounts using a trace of mineral oil and cooled in-situ to 150 K

Please cite this article in press as: E.A. Weerawardhana et al., Inorg. Chim. Acta (2016), http://dx.doi.org/10.1016/j.ica.2016.06.039

for **1** and 100 K for **2**–**5**. For **2**, frames were collected, reflections were indexed and processed, and the files scaled and corrected for absorption using APEX2 [24]. For **1** and **3**–**5**, data were collected using the Collect software [25], processed using HKL3000 and the data were corrected for absorption and scaled using Scalepack [26]. The space groups were assigned and the structures were solved by direct methods using XPREP within the SHELXTL suite of programs [27,28] and refined by full matrix least squares against $F^2$ with all reflections using SHELXL2013 or 2014 [29,30]. H atoms attached to carbon and nitrogen atoms and hydroxyl hydrogens were positioned geometrically and constrained to ride on their parent atoms, with carbon hydrogen bond distances of 0.95 Å for alkene and aromatic C-H, 1.00, 0.99 and 0.98 Å for aliphatic C-H, $CH_2$ and $CH_3$, 0.88 for N-H and 0.84 Å for OH moieties, respectively. Methyl and hydroxyl H atoms were allowed to rotate but not to tip to best fit the experimental electron density. $U_{iso}$(H) values were set to a multiple of $U_{eq}$(O/C/N) with 1.5 for $CH_3$ and OH, and 1.2 for C-H, $CH_2$ and N-H units, respectively.

Compound **3** exhibits pseudo-inversion symmetry. Exact symmetry is broken by the chiral C atoms C19, C44, C69 and C94. Refinement in P $\bar{1}$ with disorder yields R1 values larger than 15%. A toluene molecule was refined as disordered over two orientations. The less occupied moiety was restrained to have a geometry similar to that of another toluene molecule in the structure, and Uij components of ADPs of the less prevalent atoms were restrained to be similar if closer than 1.7 Å. Subject to these conditions the occupancy ratio refined to 0.835(11) to 0.165(11).

Crystal data and details of data collection **1**–**5** are given in Table S1.

## 3. Results and discussion

### 3.1. Synthesis and characterization

The asymmetric *N*-alkyl,*N*′-aryl-β-diketimine ligand (HL) was prepared in two condensation steps (Scheme 1). *N*-aryl-substituted β-ketoimine was prepared by simple condensation of diisopropylaniline and excess of 2,4-pentanedione in refluxing benzene. The desired β-diketimine ligand was synthesized by reacting the β-ketoimine with (S)-(-)-1-phenylethylamine in refluxing toluene. Although both are condensation reactions, a higher temperature was required for the second step due to the refractory nature of β-ketoimines [31]. To improve the yield for the second step, several methods were employed including treating with strong Lewis acids and *O*-alkyl agents like triethyloxonium tetrafluoroborate and dimethylsulfate. However, only intractable products were obtained from these reactions. Finally, reversing the order of the two steps led to unreacted *N*-alkyl-substituted β-ketoimine, when treated with diisopropylaniline.

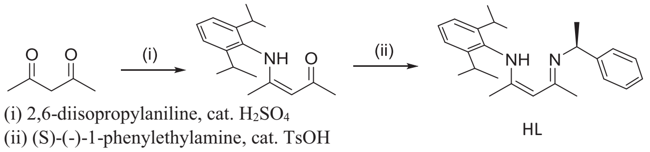

(i) 2,6-diisopropylaniline, cat. $H_2SO_4$
(ii) (S)-(-)-1-phenylethylamine, cat. TsOH

**Scheme 1.** Synthesis of N-alkyl,N′-aryl β-diketiminate β-diketimine.

Deprotonation of HL with LDA followed by transmetallation with $FeCl_2 \cdot THF_{1.5}$ and $CoCl_2$ led to iron(II) and cobalt(II) complexes (Scheme 2), respectively. Interestingly, instead of yielding 'ate' complexes $LMCl_2Li(ether)_2$ [30,31] in ethereal solvents, solvent-free chloro-bridged dimers, $[LFe(\mu\text{-Cl})]_2$ (**1**) and $[LCo(\mu\text{-Cl})]_2$ (**2**) were obtained in high yield. In addition, unlike complexes with symmetrical *N*,*N*′-diaryl β-diketiminate ligands which generally show only poor solubility in organic solvents, **1** and **2** were readily soluble in non-polar solvents, even in *n*-pentane.

Both the iron(II) and cobalt(II) complexes have paramagnetically shifted $^1$H NMR spectra. While the spectroscopic features of both **1** and **2** are in good agreement with previous observations for $[L^{Me,Dipp}Fe(\mu\text{-Cl})]_2$ [34] and $[L^{Me,Dipp}Co(\mu\text{-Cl})]_2$ ($L^{Me,Dipp}$ = 2,4-bis(2,6-diisopropylphenylimido)pentane; $L^{Me,Xyl}$ = 2,4-bis(2,6-dimethylphenylimido)pentane) [35], the $C_s$ symmetry ligand makes the resonances in the $^1$H NMR spectra difficult to assign. Solution magnetic moments (Evans method) in $C_6D_6$ for both **1** and **2** are 6.3(4) and 5.9(3) $\mu_B$, respectively, consistent with tetrahedral high-spin ions.

Crystals of **1** and **2** suitable for X-ray diffraction were obtained from a concentrated *n*-pentane solution, and their solid state structures were determined using X-ray diffraction. Selected bond distances and bond angles of complexes are listed in Table 1. The structure of **1** (Fig. 2) revealed that each iron center adapts a distorted tetrahedral coordination environment, and is analogue to $[L^{Me,Dipp}Fe(\mu\text{-Cl})]_2$ with comparable average Fe–N (1.994(3) Å) and Fe–Cl (2.380(1) Å) bond distances [32]. Similarly, the cobalt (II) ion exhibits a distorted tetrahedral geometry in **2** (Fig. S1), and shows average Co–N (1.938(4) Å) and Co–Cl (2.333(1) Å) bond distances similar to those reported for $[L^{Me,Dipp}Co(\mu\text{-Cl})]_2$ [33].

Chemical reduction of complexes **1** or **2** with $KC_8$ in the presence of excess of *cis*-cyclooctadiene gave highly air- and moisture sensitive LFe(cod) (**3**) and LCo(cod) (**4**) (Scheme 2). Sharp resonances observed in the paramagnetic $^1$H NMR spectra and the solution magnetic moments suggest high-spin iron(I) (3.8(3) $\mu_B$, $S = 3/2$) and high-spin cobalt(I) (3.2(4) $\mu_B$, $S = 1$) ions in **3** and **4**, respectively [36,37]. Crystals of both **3** (Fig. 3) and **4** (Fig. S2) suitable for X-ray diffraction were obtained from concentrated *n*-pentane solutions. Selected bond distances and angles are reported in Table 1. Compounds **3** and **4** are rare examples of low-valent iron and cobalt complexes coordinated with nitrogen donor ligands and alkene(s) [34,38,39]. The molecular geometry of the metal ion in **3** and **4** is best described as distorted tetrahedral. Each alkene has an $\eta^2$ binding mode, interacting with the metal center, and the metal distances to each carbon atom of the double bond are comparable. It should be noted that the average

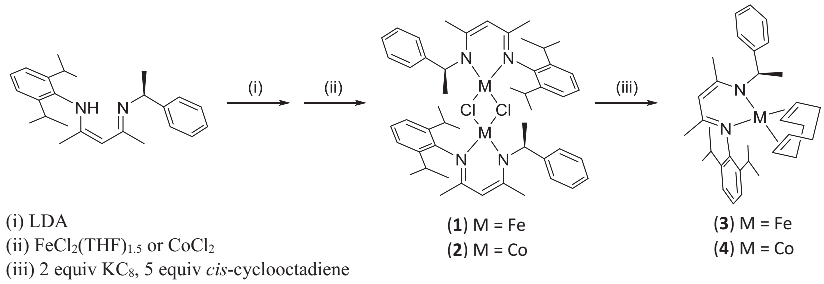

(i) LDA
(ii) $FeCl_2(THF)_{1.5}$ or $CoCl_2$
(iii) 2 equiv $KC_8$, 5 equiv *cis*-cyclooctadiene

**Scheme 2.** Synthesis of M(II) and M(I) complexes; where M = Fe and Co.

Please cite this article in press as: E.A. Weerawardhana et al., Inorg. Chim. Acta (2016), http://dx.doi.org/10.1016/j.ica.2016.06.039

**Table 1**
Selected bond distances (Å) and angles (°) in complexes **1**–**5**. Average values were listed if multiple crystallographically independent molecules existed.

| | 1 | 2 | 3 | 4 | 5 |
|---|---|---|---|---|---|
| M-N | 1.994(3) | 1.941(3) | 2.037(4) | 2.001(3) | 2.011(4) |
| | 1.993(3) | 1.935(3) | 2.038(5) | 1.974(3) | 2.005(4) |
| M-Cl | 2.374(1) | 2.327(1) | | | 2.421(2) |
| | 2.387(1) | 2.339(1) | | | 2.442(2) |
| M-O | | | | | 1.991(4) |
| | | | | | 1.988(4) |
| M-C (average) | | | 2.139(5) | 2.141(4) | |
| C=C (average) | | | 1.392(8) | 1.377(6) | |
| M···M | 3.3801(6) | 3.2304(8) | | | 3.2456(11) |
| N-M-N | 89.62(3) | 99.74(3) | 93.70(18) | 98.68(13) | 94.33(18) |
| | 89.45(3) | 100.07(14) | | | 94.08(18) |
| Cl-M-Cl | 94.65(11) | 92.91(4) | | | 83.75(5) |
| | 95.51(11) | 91.74(4) | | | |
| O-M-O | 94.65(11) | 92.91(4) | | | 109.28(18) |
| | 95.51(11) | 91.74(4) | | | |

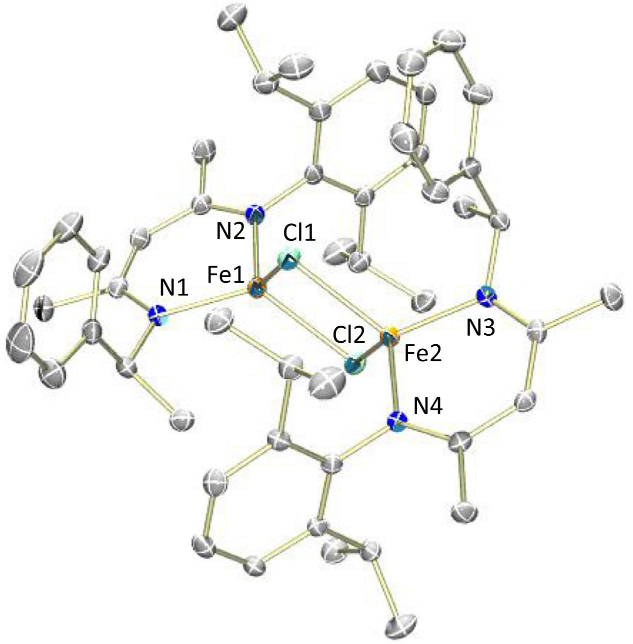

**Fig. 2.** Molecular structure of $[\mathrm{LFe}(\mu\text{-Cl})]_2$ (**1**). Hydrogen atoms are omitted for clarity. Color code: N, blue; C, gray; Fe, orange; Cl, green. Selected interatomic distances and angles are listed in Table 1. (For interpretation of the references to color in this figure legend, the reader is referred to the web version of this article.)

Fe–N (2.038(4) Å) bond distance in **3** is slightly longer than those reported for alkene-iron(I) supported by the *N*,*N*′-diaryl-substituted β-diketiminate $\mathrm{L}^{\mathrm{Me,Dipp}}$ (1.967(2) to 2.001(2) Å).

As shown in Table 1, all of the C=C double bonds in the *cis*-cyclooctadiene ligand are slightly elongated from the typical $sp^2$-$sp^2$ double bond value (1.34 Å). Comparison of the C=C bond distances of *cis*-cyclooctadiene in **3** and **4** revealed shorter C=C bond distances in **4**, suggesting a reduced π back-bonding interaction from cobalt(I). This result can be elucidated by the smaller overlap of metal *d* orbitals and alkene $\pi^*$ orbitals for cobalt than for iron. The same trend was observed for metal carbonyl complexes [40].

The yields for **3** and **4** are moderate, which could be due to their highly reactive nature toward trace amounts of water. For instance, the μ-Cl,μ-OH complex **5** was isolated as one of the by-products from the reduction of **1** [41]. A broad O-H stretching (~3500 $\mathrm{cm}^{-1}$) was observed by IR spectroscopy. The molecular structure of **5** is displayed in Fig. 4. Each iron metal presents a distorted tetrahedral environment with a chloro and a hydroxo group bridging the two iron centers. To the best of our knowledge, **5** is the first example of a chloro, hydroxo-bridged diiron complex. Both Fe-N (2.008(4) Å) and Fe-Cl (2.432(2) Å) bond distances are slightly longer than those in **1**, whereas the Cl-Fe-Cl angle is *ca.*10° smaller than that in **1**. In addition, the distance between the two Fe(II) atoms in this complex is ~0.14 Å shorter than that observed in **1**, because of the smaller bridging O atom in **5**.

### 3.2. Steric and electronic comparison

The modification of flanking groups can alter the steric and electronic profiles of supporting ligands, which in turn changes the reactivity of metal complexes [42]. With well-defined examples of **1**–**4** prepared, we are interested in the comparison of *N*-alkyl,*N*′-aryl-substituted β-diketiminate, L, and *N*,*N*′-diaryl-substituted β-diketiminates, $\mathrm{L}^{\mathrm{Me,Dipp}}$ and $\mathrm{L}^{\mathrm{Me,Xyl}}$ [43], regarding their steric and electronic effects. For iron(II) and cobalt(II) complexes, the M···M distances in **1** (3.3801(6) Å) and **2** (3.2304(8) Å) are shorter than those found in $[\mathrm{L}^{\mathrm{Me,Dipp}}\mathrm{Fe}(\mu\text{-Cl})]_2$ (3.4170(4) Å) and $[\mathrm{L}^{\mathrm{Me,Dipp}}\mathrm{Co}(\mu\text{-Cl})]_2$ (3.3723(6) Å), respectively, while slightly longer than that of $[\mathrm{L}^{\mathrm{Me,Dipp}}\mathrm{Fe}(\mu\text{-Cl})]_2$ (3.3213(6) Å). This indicates that the trend of steric hindrance of ligands is $\mathrm{L}^{\mathrm{Me,Dipp}} > \mathrm{L} > \mathrm{L}^{\mathrm{Me,Xyl}}$. To further investigate the steric hindrance of ligands, the solid angle calculation, which is used to explore the steric properties of coordinating ligands, was conducted. Interestingly, the results from the solid angle calculation for these four complexes (Table 2) showed the trend of steric hindrance of ligands as $\mathrm{L} \approx \mathrm{L}^{\mathrm{Me,Dipp}} > \mathrm{L}^{\mathrm{Me,Xyl}}$. However, the calculated data for the monomer complex **3** and $[\mathrm{L}^{\mathrm{Me,Dipp}}\mathrm{Fe(I)(alkene)}]$ complexes revealed that L is a more sterically hindered ligand than $\mathrm{L}^{\mathrm{Me,Dipp}}$. As a result, the largest steric bulkiness among three β-diketiminates is $\mathrm{L}^{\mathrm{Me,Dipp}}$ followed by L, and $\mathrm{L}^{\mathrm{Me,Xyl}}$. The different calculated data observed in solid angle calculation for **1** and **3** could be attributed to the position of the methyl group in (S)-(-)-1-phenylethylamine. In **1**, the methyl group was perpendicular to the Fe···C6 vector, whereas, it pointed outward to the metal center in **3** (Fig. S3), making the methyl group in **1** closer to the first coordination sphere of the metal than in **3**.

The electron density on the metal center can be affected by supporting ligands. The extent of the electron donation is often monitored by the CO stretching frequencies of metal carbonyl complexes by IR spectroscopy. The CO stretching frequencies for $\mathrm{LMn(CO)_3}$ (1906, 1921 $\mathrm{cm}^{-1}$) and $\mathrm{L}^{\mathrm{Me,Dipp}}\mathrm{Mn(CO)_3}$ (1915, 1924 $\mathrm{cm}^{-1}$) indicated that L is a stronger electron donating ligand than $\mathrm{L}^{\mathrm{Me,Dipp}}$.

## 4. Conclusions

We have reported the synthesis of an asymmetric *N*-alkyl,*N*′-aryl-β-diketiminate and its Fe(II), Fe(I), Co(II), and Co(I) complexes.

Please cite this article in press as: E.A. Weerawardhana et al., Inorg. Chim. Acta (2016), http://dx.doi.org/10.1016/j.ica.2016.06.039

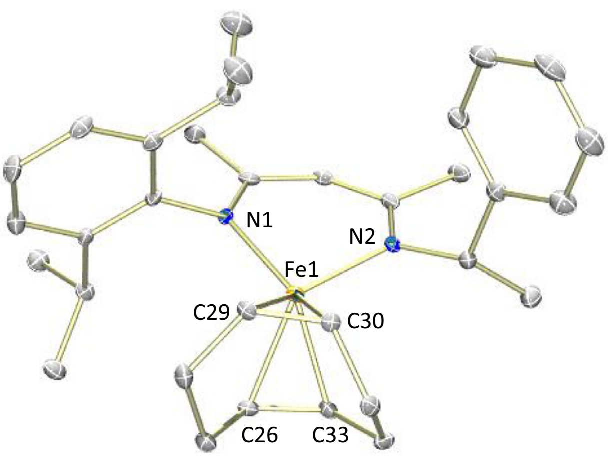

**Fig. 3.** Molecular structure of LFe(cod) (**3**). One of two crystallographically independent molecules is shown. Color code: N, blue; C, gray; Fe, orange. Hydrogen atoms are omitted for clarity. Selected interatomic distances and angles are listed in Table 1. (For interpretation of the references to color in this figure legend, the reader is referred to the web version of this article.)

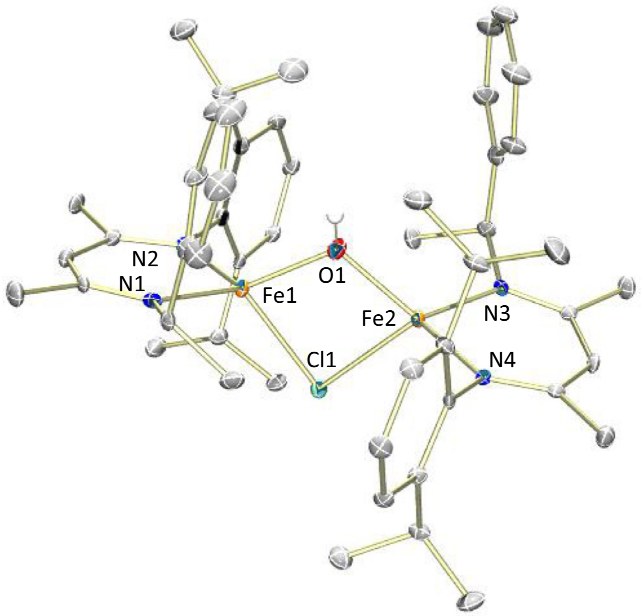

**Fig. 4.** Molecular structure of LFe(μ-Cl)(μ-OH)FeL (**5**). One of two crystallographically independent molecules is shown. Color code: N, blue; C, gray; O, red; Fe, orange. Hydrogen atoms are omitted for clarity. Selected interatomic distances and angles are listed in Table 1. (For interpretation of the references to color in this figure legend, the reader is referred to the web version of this article.)

**Table 2**
Solid angle data (*G*) for complexes **1**–**4** and selected complexes with *N*,*N*′-diaryl-β-diketiminates.

| Ligand | Fe(II) | Co(II) | Fe(I) | Co(I) |
|---|---|---|---|---|
| L | 53.22 | 53.13 | 50.12 | 46.86 |
| $L^{Me,Dipp}$ | 52.83[a] | 52.62[c] | 55.98[d]<br>56.81[d] | NA |
| $L^{Me,Xyl}$ | 49.24[b] | NA | | NA |

[a] Ref. [34].
[b] Ref. [42].
[c] Ref. [35].
[d] Ref. [36].

All four complexes have been characterized by $^1$H NMR spectroscopy, elemental analysis, and were crystallographically authenticated. Crystallographic and spectroscopic results indicate that the *N*-alkyl,*N*′-aryl-β-diketiminate ligand L is sterically smaller but a better electron donor than the *N*,*N*′-diaryl-substituted β-diketiminate ligand $L^{Me,Dipp}$. Reactivity studies on the highly reactive compounds **3** and **4** are currently being pursued.

## Acknowledgment

Funding was provided by College of Arts and Sciences at Loyola University Chicago. NSF REU Program (Research Experience for Undergraduates) is gratefully acknowledged for summer financial support for A.P. The Bruker Quest X-ray diffractometer was funded by NSF Grant DMR 1337296. We thank Dr. Phillip Fanwick at Purdue University for his assistance in collecting crystallographic data of **1**.

## Appendix A. Supplementary data

CCDC 1484031–1484035 contain the supplementary crystallographic data for **1**–**5**. These data can be obtained free of charge from The Cambridge Crystallographic Data Centre via http://www.ccdc.cam.ac.uk/data_request/cif. Supplementary data associated with this article can be found, in the online version, at http://dx.doi.org/10.1016/j.ica.2016.06.039.

## References

[1] J.E. Parks, R.H. Holm, Inorg. Chem. 7 (1968) 1408.
[2] L. Bourget-Merle, M.F. Lappert, J.R. Severn, Chem. Rev. 102 (2002) 3031.
[3] P.L. Holland, Acc. Chem. Res. 41 (2008) 905.
[4] Y.-C. Tsai, Coord. Chem. Rev. 256 (2012) 722.
[5] K.-H. Park, W.J. Marshall, J. Am. Chem. Soc. 127 (2005) 933.
[6] B. Sedai, M.J. Heeg, C.H. Winter, Organometallics 28 (2009) 1032.
[7] F. Drouin, P.O. Oguadinma, T.J.J. Whitehorne, Organometallics 29 (2010) 2139.
[8] D. Li, Y. Peng, C. Geng, K. Liu, D. Kong, Dalton Trans. 42 (2013) 11295.
[9] E. Shaviv, M. Botoshansky, M.S. Eisen, J. Organomet. Chem. 683 (2003) 165.
[10] S.B. Cortright, J.N. Coalter, M. Pink, J.N. Johnston, Organometallics 23 (2004) 5885.
[11] M.M. Rodriguez, E. Bill, W.W. Brennessel, P.L. Holland, Science 334 (2011) 780.
[12] S. Yao, M. Driess, Acc. Chem. Res. 45 (2012) 276.
[13] S. Wiese, M.J.B. Aguila, E. Kogut, T.H. Warren, Organometallics 32 (2013) 2300.
[14] S. Gong, H. Ma, J. Huang, J. Organomet. Chem. 693 (2008) 3509.
[15] M. Schmid, S.M. Guillaume, P.W. Roesky, Organometallics 33 (2014) 5392.
[16] M. Biyikal, K. Löhnwitz, N. Meyer, M. Dochnahl, P.W. Roesky, S. Blechert, Eur. J. Inorg. Chem. (2010) 1070.
[17] C.-H. Wang, C.-Y. Li, B.-H. Huang, C.-C. Lin, B.-T. Ko, Dalton Trans. 42 (2013) 10875.
[18] C.-H. Wang, C.-Y. Li, C.-H. Lin, Y.-C. Liu, B.-T. Ko, Inorg. Chem. Commun. 14 (2011) 1456.
[19] Y. Lv, C.E. Kefalidis, J. Zhou, L. Maron, X. Leng, Y. Chen, J. Am. Chem. Soc. 135 (2013) 14784.
[20] W.C. Ellis, Y. Jung, M. Mulzer, R. Di Girolamo, E.B. Lobkovsky, G.W. Coates, Chem. Sci. 5 (2014) 4004.
[21] A.P. Dove, V.C. Gibson, E.L. Marshall, A.J.P. White, D.J. Williams, Dalton Trans. (2004) 570.
[22] E.M. Schubert, J. Chem. Educ. 69 (1992) 62.
[23] I.A. Guzei, M. Wendt, Dalton Trans. (2006) 3991.
[24] Apex2 v2009.7-0, Bruker AXS Inc.: Madison (WI), USA; 2009.
[25] R.W.W. Hooft, Collect, Nonius BV, Delft, The Netherlands, 1998.
[26] Z. Otwinowski, W. Minor, Methods Enzymol. 276 (1997) 307.
[27] SHELXTL (Version 6.14) (2000–2003) Bruker Advanced X-ray Solutions, Bruker AXS Inc., Madison, Wisconsin: USA.
[28] G.M. Sheldrick, Acta Cryst. A64 (2008) 112.
[29] G.M. Sheldrick, Acta Cryst. C71 (2015) 3.
[30] G.M. Sheldrick, University of Göttingen Germany, 2013.
[31] A.Z. Bradley, D.L. Thorn, G.V. Glover, J. Org. Chem. 73 (2008) 8673.
[32] J.M. Smith, R.J. Lachicotte, P.L. Holland, Chem. Commun. (2001) 1542.
[33] E. Bernoud, P. Oulié, R. Guillot, M. Mellah, J. Hannedouche, Angew. Chem. Int. Ed. 53 (2014) 4930.
[34] N.A. Eckert, J.M. Smith, R.J. Lachicotte, P.L. Holland, Inorg. Chem. 43 (2004) 3306.
[35] W. Gao, Y. Mu, G.-H. Li, X.-M. Liu, Q. Su, W. Yao, Chem. Res. Chin. Univ. 21 (2005) 240.
[36] Y. Yu, J.M. Smith, C.J. Flaschenriem, P.L. Holland, Inorg. Chem. 45 (2006) 5742.

Please cite this article in press as: E.A. Weerawardhana et al., Inorg. Chim. Acta (2016), http://dx.doi.org/10.1016/j.ica.2016.06.039

[37] M.H. Al-Afyouni, E. Suturina, S. Pathak, M. Atanasov, E. Bill, D.E. DeRosha, W.W. Brennessel, F. Neese, P.L. Holland, J. Am. Chem. Soc. 137 (2015) 10689.
[38] G. Bai, P. Wei, A.K. Das, D.W. Stephan, Dalton Trans. (2006) 1141.
[39] J.D. Jewson, L.M. Liable-Sands, G.P.A. Yap, A.L. Rheingold, K.H. Theopold, Organometallics 18 (1999) 300.
[40] M. Zhou, L. Andrews, C.W. Bauschlicher, Chem. Rev. 101 (2001) 1931.
[41] Due to the small quantity of product, 5 has not been fully characterized.
[42] C. Chen, S.M. Bellows, P.L. Holland, Dalton Trans. 44 (2015) 16654.
[43] K. Grubel, W.W. Brennessel, B.Q. Mercado, P.L. Holland, J. Am. Chem. Soc. 136 (2014) 16807.

Please cite this article in press as: E.A. Weerawardhana et al., Inorg. Chim. Acta (2016), http://dx.doi.org/10.1016/j.ica.2016.06.039